Resistive Interchange Modes in Negative Central Shear Tokamaks with Peaked Pressure Profiles

M. S. Chu,[1] J. M. Greene,[1] L. L. Lao,[1] R. L. Miller,[1] A. Bondeson,[2] O. Sauter,[3,*] B. W. Rice,[4,†] E. J. Strait,[1] T. S. Taylor,[1] and A. D. Turnbull[1]
[1]*General Atomics, San Diego, California 92186-9784*
[2]*Institute for Electromagnetic Field Theory, Chalmers University, Göteborg, Sweden*
[3]*CRPP/EPFL, Assoc. EURATOM-Switzerland, Lausanne, Switzerland*
[4]*Lawrence Livermore National Laboratory, Livermore, California*
(Received 20 May 1996)

Resistive interchange modes can be driven unstable by large pressure gradients in the negative central magnetic shear (NCS) region of advanced tokamaks. Localized stability analysis reveals that the resistive interchange stability criterion ($D_R \leq 0$) is violated in this region, and unstable $n = 1$ localized resistive magnetohydrodynamic (MHD) modes are computed using the resistive MHD code MARS. In DIII-D NCS plasmas, these instabilities appear as bursting MHD activities, constituting the first identification of resistive interchange in a high temperature tokamak experiment. These bursts also appear to play a role in triggering disruptions. [S0031-9007(96)01253-7]

PACS numbers: 52.50.Gj, 52.55.Fa

Negative central magnetic shear (NCS) is an operating regime [1–3] for advanced tokamaks which could lead to fusion reactors with higher performance and lower cost. In the NCS region, the plasma is in the second stable regime for ideal magnetohydrodynamic (MHD) ballooning modes. In Tokamak Fusion Test Reactor (TFTR) and DIII-D, the plasma also develops an internal transport barrier [4,5] that provides good central confinement, high central ion temperatures, and central peaking of the pressure profile—favorable for a high fusion rate [6,7]; record high neutron yield has been obtained in peaked pressure operations. In *L*-mode plasmas, i.e., no edge pressure pedestal, these discharges typically terminated with hard disruptions. Despite the favorable ballooning mode stability cited above, localized MHD bursts are observed in plasmas with highly peaked pressure profile in DIII-D. These bursts limit the pressure peakness $p(0)/\langle p\rangle$ [$p(0)$ is the pressure at the plasma center and $\langle p\rangle$ is the volume-averaged pressure], and occur prior to the final disruption. In what follows, these bursts will be identified as manifestations of the resistive interchange instability.

Resistive instabilities in general toroidal plasma configurations were first analyzed by Glasser, Greene, and Johnson [8]. They predicted the existence of a class of resistive MHD modes localized to resonant surfaces where magnetic lines are closed, or $m = nq$ (here m, n are the poloidal and toroidal mode numbers and q the safety factor or winding number) when the resistive localized interchange stability criterion $D_R \leq 0$ is violated. Although this criterion has been known for some time, the resistive interchange has not been observed to date. In this Letter, we show that in NCS configurations with peaked pressure profiles, not only can the localized criterion $D_R \leq 0$ be violated, but explicit $n = 1$ modes can be identified using the resistive MHD code MARS [9,10]. We also show that the parameter space in which these instabilities are found, as well as the mode structure, agrees quantitatively with that observed in the DIII-D experiment. These constitute the first positive identification of the resistive interchange in a high temperature tokamak experiment.

To investigate the parametric dependence of the resistive localized interchange in NCS configurations, we generated a set of equilibria by using the TOQ equilibrium code [11] and corresponding to those obtained in DIII-D. The aspect ratio is fixed at 2.7, the elongation is 1.8, and the triangularity is 0.7. The q profile is specified by a spline with the value of $q_{\min}$ covering a range from 1.1 to 2.5. The value of $q_0 - q_{\min}$ ranges from -0.3 to 1 (a negative value of $q_0 - q_{\min}$ corresponds to normal q profile with the minimum value of q at the magnetic axis). The pressure profile is given by the form $p = p_0(1 - \psi)^n$. With increasing value of the exponent n, the pressure profile becomes more peaked. The equilibria studied cover a range of $\beta_N = \beta(I_p/aB_0)^{-1}$ (% MA/mT) values between 0.5 and 5.0 (here $\beta = 2\mu_0\langle p\rangle/B_0^2$ is the ratio of plasma pressure to magnetic field pressure, I_p is plasma current, a the plasma minor radius, and B_0 the vacuum magnetic field).

We first describe the localized stability of these equilibria. They are always stable to the ideal interchange even in the absence of magnetic shear ($D_I < -1/4$) and also stable to the ideal ballooning modes. However, the localized resistive interchange is destabilized at sufficiently high β_N. Note that D_R is connected to the ideal interchange stability index D_I through the relationship $D_R = D_I + (H - 1/2)^2$. Explicit expressions of D_I, D_R, and H are given in Ref. [8]. For tokamaks,

$$H = \frac{\mu_0 p' V' f}{(2\pi)^2 q'}\left[\left\langle \frac{1}{|\vec{\nabla}\psi|^2}\right\rangle - \frac{\langle B^2/|\vec{\nabla}\psi|^2\rangle}{\langle B^2\rangle}\right].$$

Here $\langle\cdots\rangle$ represents the average over the flux surface, and $\vec{B} = f\vec{\nabla}\phi + \vec{\nabla}\phi \times \vec{\nabla}\psi$, V is the volume enclosed by

 0031-9007/96/77(13)/2710(4)$10.00

the flux surface, and $'$ is differentiation with respect to ψ. H is a quantity inversely proportional to magnetic shear and directly proportional to the local pressure gradient of the particular surface. For tokamaks with a normal (positive) shear profile and small pressure gradient, H is small and positive, and D_R is slightly less than $D_I + 1/4$. In regions of NCS, H is always negative. Although $D_I + 1/4$ remains negative, D_R gradually becomes positive as the β value is increased. In Fig. 1 is shown (a) the typical q profile, (b) the dependence of D_R on the degree of reversal $[q(0) - q_{\min}]$, and (c) the dependence of D_R on β_N. We note that these trends shown in this numerical evaluation of D_R are in agreement with the large aspect ratio analytic results for tokamaks with circular [12] and noncircular [9] cross sections. Thus the resistive interchange is the only localized MHD instability that can exist in the NCS region of a finite beta plasma, and this instability occurs only beyond a threshold β_N value.

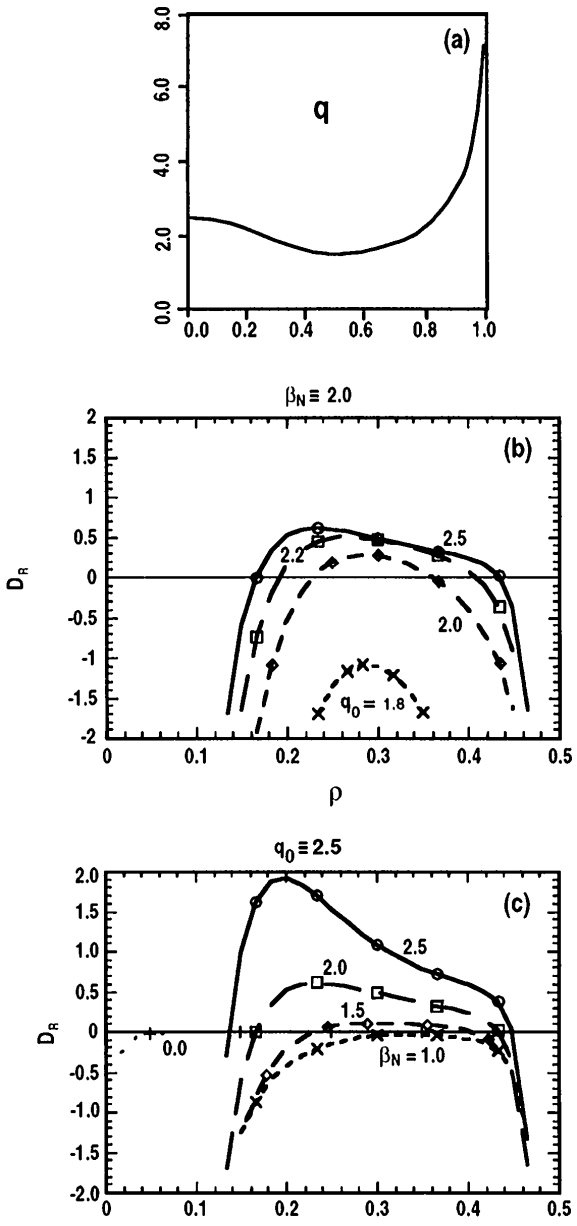

FIG. 1. (a) shows a typical reversed q profile. In here $q_{\min} = 1.5$ located at $\rho = 0.5$. The resistive interchange is destabilized by increasing q_0 (shear reversal) shown in (b) with β_N fixed at 2.0. It is also destabilized by increasing β_N shown in (c) with q_0 fixed at 2.5.

Next we describe the mode structure and stability threshold of these instabilities using the resistive MHD stability code MARS [9]. MARS solves the full set of linearized resistive MHD equations including the effect of a subsonic toroidal plasma flow [10] (although the equilibria does not include rotation). In these calculations, the toroidal mode number n has been taken to be $n = 1$. A set of unstable MHD modes localized around q rational surface in the reverse shear region (satisfying $m = nq$ with m being an integer) is clearly identifiable when $D_R > 0$ over a region around this singular surface. The perturbed radial velocity δv_r on the mode resonant surface is nearly constant along field lines. The magnetic perturbation δb_r, however, has its amplitude dominated by the residual variation of the radial displacement. (We note that interchange modes are even in δv_r and odd in δb_r across the resonant surface.) A typical plot of the amplitudes for an equilibrium with $q_{\min} = 1.5$ and $\beta_N = 3.3$ is given in Fig. 2 for δv_r. Note that δv_r is quite localized to the mode resonant surface. This feature is especially noticeable when β_N increases so that another more global mode is also excited. The $n = 1$ localized mode is also found to be destabilized beyond a certain β_N value β_{Nc}, indicating that these modes are pressure driven interchanges. The β_{Nc} found from MARS is higher than that given by the localized criterion $D_R \geq 0$, due to the fact that the $n = 1$ mode first appears only if the localized criterion is violated over a range of the flux surfaces around the mode rational surface. The dependence of the growth rate γ on the value of the plasma resistivity η

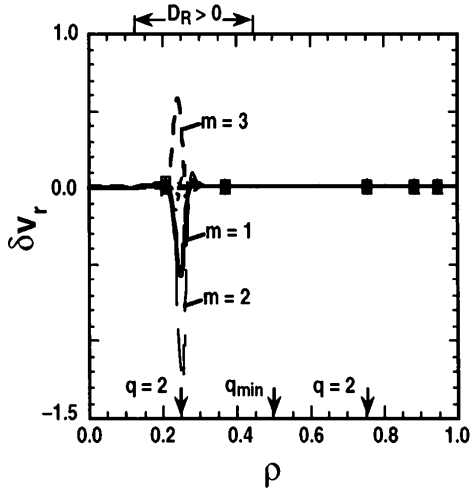

FIG. 2. Typical computed mode structure of the perturbed radial velocity δv_r. The poloidal mode number is based on an equal arc grid.

is further evidence for the identification of these modes; we find at small η, γ decreases as $\eta^{1/3}$ as predicted by Glasser, Greene, and Johnson [8]. The growth rate is also found to be independent of the plasma rotation. With increasing plasma rotation, the mode rotates with the rotation speed of the singular surface in the reverse shear region with no change in its growth rate. Both the growth rate and the mode structure are insensitive to the location of the external conducting wall.

The dependence of β_{Nc} on some of the key equilibrium parameters was also studied. The localized mode is not found when the $q_0 - q_{\min}$ is small or negative, due to the fact the D_R is not sufficiently positive over the region near the singular surface. On the other hand, with $q_0 - q_{\min}$ fixed (at 1), β_{Nc} has been found to be insensitive to the value of $q_{\min}$. The computed value of this is shown as the solid line in Fig. 3. Varying the pressure peakedness parameter $p(0)/\langle p\rangle$ while keeping $q_0 - q_{\min}$ fixed (at 1), we found that β_{Nc} decreases strongly with increasing $p(0)/\langle p\rangle$. This dependence is shown as the solid line in Fig. 4.

The calculated resistive interchange instability (in these NCS equilibria) agrees well with the MHD activity observed in high beta DIII-D discharges with negative central shear and strongly peaked pressure profiles. In these discharges, an internal transport barrier leads to large pressure gradients in the NCS region [6,7]. The central pressure and volume-average beta rise steadily until a disruption occurs [Fig. 5(a)]. The disruption is often preceded by one or more bursts of MHD activity which we here identify as the resistive interchange mode. The bursts of MHD activity usually observed in the last 50 ms before the disruption are shown in Fig. 5(b). These bursts have a mode number $n = 1$ and a growth time 0.1 to 0.5 ms, one to two orders of magnitude faster than the typical growth of resistive instabilities near the ideal beta limit but an order of magnitude slower than that observed for ideal kink modes at the beta limit. The mode saturates at a relatively low amplitude.

The evidence that the bursting instability is the predicted resistive instability is as follows: Motional Stark effect measurements of the profile of the local B show a decrease at small minor radius and an increase at large minor radius following the burst, implying a flattening of the q profile in the negative shear region. Charge exchange recombination data show a similar flattening of the rotation and pressure profile. These profile measurements, as well as the mode rotation frequency, indicate a radial location near the magnetic axis. Detailed modeling of soft x-ray data in different discharges is consistent with an $m = 3$ mode near the magnetic axis, at the location of the $q = 3$ surface in the strong negative shear region. For strongly peaked pressure profiles, the disruptions occur at relatively low values of β_N, between 1.8 and 2.3. The disruption threshold is constant for $1.3 \leq q_{\min} \leq 3$, suggesting that the beta limit is not related to the low shear region near $q_{\min}$. Although the disruption itself appears to be the result of a different, more global instability, quantitative threshold of β_N and its independence on $q_{\min}$ agree very well with predictions for the resistive interchange mode. For comparison, the experimental values of β_N at disruption are shown as heavy dots in Fig. 3. We also note that these bursts are not observed in weakly reversed shear discharges, in agreement with predictions of theory. Furthermore, disruptions can be avoided at much higher β_N by broadening the pressure profile, again consistent with predictions for the resistive interchange mode. Discharge time histories of several discharges are shown as dotted lines in Fig. 4 and compared with the predicted stability boundary of the resistive interchange mode. It is seen that in H-mode discharges with the edge pressure

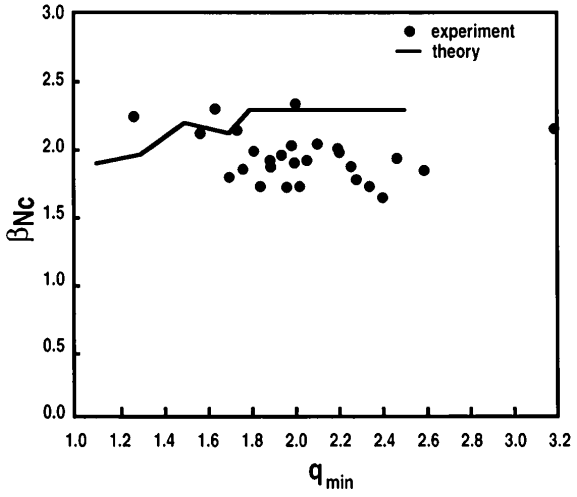

FIG. 3. Instability threshold in β_N versus $q_{\min}$. The solid line is results calculated for the resistive interchange mode using the set of simulated equilibria. The dots are experimentally observed values in DIII-D discharges with peaked pressure profiles.

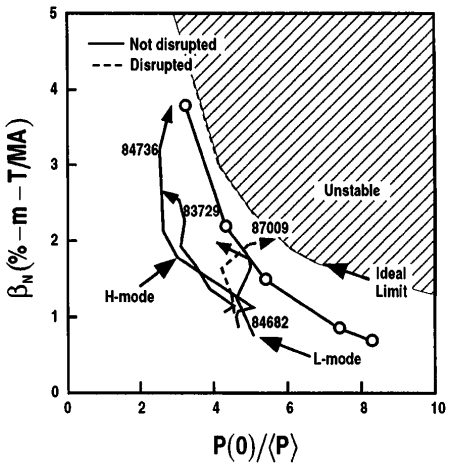

FIG. 4. Calculated threshold in β_N versus $p(0)/\langle p\rangle$ for the resistive interchange mode, with trajectories of stable and unstable experimental discharges.

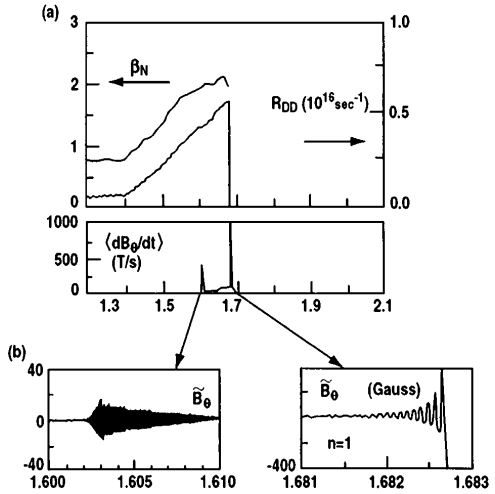

FIG. 5. Time traces of shot 87009. (a) Time traces during the high beam power phase, including beam power, beta, neutron rate, and δB amplitude; (b) time expansion of δB signal during a burst.

pedestal, where the plasma develops a broader peaked pressure profile, the discharge history lies within the stability boundary. In *L*-mode discharges, when the plasma develops a peaked pressure profile, its trajectory in the stability space encroaches into the unstable region and the plasma disrupts. The experimental equilibria in this case have been reconstructed by using the EFIT [13] equilibrium code. The resistive interchange is found for the equilibrium as its trajectory crosses the expected stability boundary; both resistive interchange and another global mode are found for the equilibrium at the later time of disruption. We see that the DIII-D experiment is in a parameter space where these two modes are expected to interact strongly with each other. The localized mode regulates the pressure profile whereas the global mode leads to disruption.

Although the computed growth rate based on experimental magnetic Reynolds number is too low to account for the measured experimental growth rate, it is difficult to identify the mode not as a resistive interchange but as a resistive or kinetic (high n) ballooning mode [14] because only low n ($= 1$) magnetic perturbations have been observed. We note that there is substantial rotation present in the experiment. This might affect the equilibrium and provide some additional driving force to enhance the growth rate. $n = 2$ or higher resistive interchanges have also been computed by MARS but only occasionally observed in the experiment. They could also have been stabilized by kinetic effects not taken into account in the fluid theory. Furthermore, there is substantial uncertainty in the equilibrium reconstruction that could affect the coupling of the resistive interchange with the global mode. It is also possible that the experimental observation is in a nonlinear regime in which nonlinear effects enhance the growth rate. Without further complicating the issues, we limit our present discussion based on the linear resistive MHD model and defer further discussion of this discrepancy until the issue of rotation and nonlinear effect has been systematically investigated.

We conclude from the above comparison that the bursting MHD activity observed near the disruption boundary of NCS discharges in DIII-D is caused by the resistive interchange modes. These modes give rise to local relaxation of the pressure, rotation, and q profiles. The stability boundary of this mode closely resembles that for the observed disruptions. Calculations with MARS show increased coupling of the resistive interchange mode to a double tearing mode at high beta, providing a possible means for destabilizing a more global mode. This mode may be avoided by employing broader pressure profiles and weaker shear reversal, indicating possible avenues for the optimization of NCS operation.

The authors acknowledge stimulating discussions with V. S. Chan, T. H. Jensen, and E. A. Lazarus.

This is a report of work sponsored by the U.S. Department of Energy under Grant No. DE-FG03-95ER54309 and Contract No. W-7405-ENG-48, and supported in part by the Swiss National Science Foundation.

*Present address: ITER Site, La Jolla, California 92037.
†Present address: General Atomics, San Diego, California 92186-9784.

[1] T. S. Taylor *et al.*, Plasma Phys. Controlled Fusion **36**, B229 (1994).
[2] C. Kessel *et al.*, Phys. Rev. Lett. **72**, 1212 (1994).
[3] A. D. Turnbull *et al.*, Phys. Rev. Lett. **74**, 718 (1995).
[4] F. M. Levinton *et al.*, Phys. Rev. Lett. **75**, 4417 (1995).
[5] E. J. Strait *et al.*, Phys. Rev. Lett. **75**, 4421 (1995).
[6] L. L. Lao *et al.*, Phys. Plasmas **3**, 1951 (1996).
[7] B. W. Rice *et al.*, Phys. Plasmas **3**, 1983 (1996).
[8] A. H. Glasser, J. M. Greene, and J. L. Johnson, Phys. Fluids **18**, 875 (1975).
[9] A. Bondeson, G. Vlad, and H. Lutjens, Phys. Fluids B **4**, 1889 (1992).
[10] M. S. Chu, J. M. Greene, T. H. Jensen, R. L. Miller, A. Bondeson, R. W. Johnson, and M. E. Mauel, Phys. Plasmas **2**, 2236 (1995).
[11] R. L. Miller and J. W. Van Dam, Nucl. Fusion **27**, 2101 (1987).
[12] A. H. Glasser, J. M. Greene, and J. L. Johnson, Phys. Fluids **19**, 567 (1976).
[13] L. L. Lao *et al.*, Nucl. Fusion **30**, 1035 (1990).
[14] A. Hirose and M. Elia, Phys. Rev. Lett. **76**, 628 (1996).